Applied Thermal Engineering 218 (2023) 119212

Contents lists available at ScienceDirect

Applied Thermal Engineering

journal homepage: www.elsevier.com/locate/ate

Research Paper

High performance blended nanofluid based on gold nanorods chain for harvesting solar radiation

Sajid Farooq [a,b,c], Diego Rativa [a,d], Zafar Said [e,f,*], Renato E. de Araujo [b]

[a] Institute of Innovation and Technology, University of Pernambuco, Recife, Brazil
[b] Laboratory of Biomedical Optics and Imaging, Federal University of Pernambuco, Recife, Brazil
[c] Center for Lasers and Applications, Instituto de Pesquisas Energéticas e Nucleares, Av. Prof. Lineu Prestes 2242, São Paulo, 05508-000, Brazil
[d] Applied Physics Program, Federal Rural University of Pernambuco, Recife, Brazil
[e] Sustainable and Renewable Energy Engineering Department, University of Sharjah, 27272, Sharjah, United Arab Emirates
[f] U.S.-Pakistan Center for Advanced Studies in Energy (USPCAS-E), National University of Sciences and Technology (NUST), Islamabad, Pakistan

ARTICLE INFO

Keywords:
Plasmonic
Metallic nanoparticles
Solar thermal collector
Direct absorption
Inhomogeneous colloid

ABSTRACT

Colloids composed of metallic nanoparticles are promising working fluids for solar radiation harvesting using Direct Absorption Solar Collectors (DASC), due to a high thermal conductivity characteristic and a broad optical absorption that can be tuned to match the solar spectrum. Recently, different studies report gold nanorod (Au-NR) chains for biosensing and photothermal applications, which have broadband and high absorption cross-section and potential possibilities to orientate the nanoparticle using electromagnetic fields. Moreover, colloids with nanoparticles blended configuration show an efficient solar radiation absorption characteristics. Here, working fluids for DASC based on gold nanorod chains in an unblended and blended configuration are evaluated using numerical simulations. The results indicate that the solar absorption increases proportional to the size of the Au-NR assembly, and the best configuration is obtained for a tetramer structure. By using different blended arrangements such as single Au monomers, dimers, trimmers, and tetramers nanorods, it is possible to obtain solar weighted absorption coefficients close to an ideal solar thermal collector, even obtained at low volume fraction (1×10^{-5}). Moreover, the results show an enhancement of the temperature of 58.45 °C for tetramer compared with a monomer structure, both under one sun excitation. Therefore, the Au-NR assembly shows a high potentiality to be explored as a high-performance working fluid for solar thermal collectors.

1. Introduction

With the thriving global warming and the substantial environmental impacts due to fossil fuels-based conventional energy sources, the urgent challenge is to overcome the energy demands with pollution-free and renewable energy for the future development of utility sectors [1,2]. Solar energy is the most plentiful and one of the cleanest and sustainable energy sources. Due to its excessive availability, it exhibits potential applications such as desalination, air conditioning, domestic hot-water provision, and electricity generation [3,4]. Among various technologies for utilizing solar energy, a direct absorber solar collector (DASC) employing base-fluids is the simplest and the most direct way that recovers the sun's energy and transfers it into heat [2,5,6].

Conventional solar thermal collectors use black surfaces to absorb solar radiation, transferring the heat to a working fluid directly or by using intermediate carrier liquids. However, their performances are limited by optical reflections and surface heating losses [2]. For instance, water has been commonly utilized as a working fluid, however, due to its limited thermo-physical features these solar collectors directly needed thermally efficient working fluid. Moreover, the energy transfer efficiency improves by absorbing the solar radiation directly by the working fluid as proposed in the DASC [7]. Therefore, nanofluids (NFs) have been examined by researchers as an alternative fluid to the water for solar energy harvesting and have been proved to increase efficiently photothermal performance [5].

Plasmonic NPs may have high absorption features at the visible-infrared spectrum region, and thermal conductivity typical of metals, satisfying two important conditions: to match well the AM1.5 solar radiation spectrum and to transfer the energy efficiently to the surrounding fluid [2,8–11]. Working fluids such as water, Therminol VP-1, ethylene, and propylene glycol absorb only 13% of the incident solar energy and have a low thermal conductivity limiting the heating performance [10]. On the other hand, nanofluids containing oil based Au NPs can achieve thermal efficiency above 24.9% [12]. Moreover, the thermal conductivity enhancement governed by the tested nanofluids

* Corresponding author at: Sustainable and Renewable Energy Engineering Department, University of Sharjah, 27272, Sharjah, United Arab Emirates.
E-mail addresses: zsaid@sharjah.ac.ae, zaffar.ks@gmail.com (Z. Said).

https://doi.org/10.1016/j.applthermaleng.2022.119212
Received 26 May 2022; Received in revised form 30 July 2022; Accepted 22 August 2022
Available online 6 September 2022

enhanced with increasing NPs loading and by tuning their geometric parameters [13].

Different designs and plasmonic structures have been proposed for applications in DASC devices, optimizing the localized surface plasmon resonance (LSPR) to harvest solar radiation with different sizes, shapes, and material composition. Moghadam et al. explored CuO nanofluid to evaluate thermal efficiency 21.8% with the volume fractions of NPs is set 0.4% (mass flow rate 1 kg/min) [14]. Employing Al_2O_3 nanofluid, it was demonstrated that the thermal efficiency enhanced 28.3% at the volume fractions 0.2 wt% [15]. Taygi et al. studied Al NPs based nanofluid and found that direct solar thermal collector possessed up to 10% higher efficiency in comparison with flat plate collector [16]. Furthermore, it is reported that the nanofluid made of TiO_2 NPs was found to increase thermal efficiency 15.7%. Filho et al. found that the presence of Ag nanoparticle in base-fluid enhanced higher photothermal conversion efficiency (144%) for very low particle concentration (6.5 ppm) in comparison to H_2O [17]. Chen et al. investigated that Au nanofluid showed better photo-thermal conversion efficiency (21.3%), compared with H_2O even at relatively low concentration (0.000008 wt%) [18].

In order to enhance the photothermal conversion efficiency of solar collectors, several geometrical parameters (e.g. shape, size and structure) of nanofluids have been tuned to harvest solar spectrum. Recently, Fontana et al. demonstrated the fabrication of stable colloidal gold nanorod (Au-NR) assembly, prepared with chemical reductions by melting with femtosecond laser welding, considering properties for sensing and photothermal applications. The Au-NR colloid has a broad LSPR spectrum and high absorption cross-section [19,20]. The NPs assembly, two or more closely spaced metallic structures, are considered as one of the primary nanoscale geometries in plasmonics, assisting robust near field enhancements in their nanogaps junction under illumination [21,22]. It was also experimentally studied that the NPs assembly absorption resonance relied linearly on the chain-length, providing the absorption response within visible to IR regime [19].

In this work, the solar collector efficiency of a working fluid composed of Au-NR chains connected with a dielectric junction material is analyzed for a monomer, dimer, trimer, and tetramer assembly, for a blended and un-blended colloid. The optical linear properties of NPs assembly are computed using Full-wave field analysis to obtain solar weighted absorption coefficient for DASC. Further, the optical absorbed power density of nanoheaters is computationally solved in stationary (time harmonic) field solution to evaluate optical–thermal conversion performance, which leads to manipulate colloidal temperature.

2. Numerical tools

2.1. Numerical analysis for optical properties

A 3-dimensional full-wave simulations model is used to explore the optical features of the NFs, employing finite element methods (FEM) in COMSOL Multiphysics. As represented in Fig. 1, the model domain is a rectangular space with a height of 2800 nm and thickness ~ 200 nm, limited by two perfectly matched layers (PML) with a thickness of 200 nm. The nanostructures analyzed are centered at the origin of the computational domain, surrounded by a water medium. In that geometry size, the mesh in the junction region of the dimer is extremely small (0.2 nm) and is segmented into tetrahedral shaped elements. Further, the maximum size of mesh was set 20 nm for surrounding domain around the metallic structure. Perfect electric (PEC) and magnetic (PMC) boundary conditions minimize reflections from the boundaries.

The Au-NR are geometrical cylinders with length $L = 42$ nm, diameter $d = 15$ nm, which area surface is segmented into small tetrahedral elements. In the case of multimer, the two hemispherical ends of the Au-NR are bridged by a thin dielectric ($n = 1.48$) junction with length $G = 1$ nm and diameter $d = 1$ nm, as represented in Fig. 1.

The optical interaction between the solar radiation (unpolarized light) and the Au-NR is analyzed with an incident E-field [1 V/m] polarized along with the primary (long and short) axis of the Au-NR array, and averaging these two calculations. The solar radiation ($\lambda = 300$ nm–1300 nm) is applied from the top surface and propagates downward towards the bottom of the computational domain. The working fluids are studied under the regime of low volume fraction ($p < 10^{-4}$), such that the inter-particle interaction is negligible, and the thermo-optical analysis can be considered for a single NP.

Johnson & Christy reported the gold permittivity values for bulk [23], and the size dependence correction for small particles where the electron-interface scattering is significant, given by [24]:

$$\epsilon(\omega, L_{eff}) = \epsilon_{bulk}(\omega) + \frac{{\omega_p}^2}{\omega^2 + i\omega\gamma_0} - \frac{{\omega_p}^2}{\omega^2 + i\omega(\gamma_0 + AV_f/L_{eff})}, \quad (1)$$

where ω_p represents plasma frequency, V_f is the Fermi velocity, γ_0 denotes a phenomenological scattering parameter that describes the scattering of the electrons with phonons, electrons, lattice defects, or impurities in a bulk material. For gold, these values are given as $\gamma_0 = 1.07 \times 10^{14}$ s^{-1} and $V_f = 1.40 \times 10^6$ ms^{-1} [25]. Here, A is a dimensionless parameter and closes to unity. Moreover, L_{eff} is the effective electron path length, given by $L_{eff} = 4V/S$ where V is the NP volume and S is the surface area [26].

The numerical model, as well as the methodology, is validated with the light interaction results obtained using Mie theory for single nanorod [27].

2.2. Heat study

We investigate the plasmonics assisted heat analysis of the Au-NR assembly using FEM computational model. The modules, both, heat transfer and RF are coupled to obtain the thermal characteristics of the plasmonic nanoparticles. The optical absorbed power density Q i.e. the heat induced per unit volume of the nanostructure Q_h (W/m^3) is computationally solved in stationary (time harmonic) field solution in RF modeling and act as a heating source in thermal model. The temperature during the whole computational domain fulfills the equation [28]:

$$\rho C_p \frac{\partial T}{\partial t} + \nabla \cdot (-k\nabla T) = Q \quad (2)$$

where ρ is heat density of water, C_p is the heat capacity at constant pressure and κ is thermal conductivity. Moreover, Q is thermal energy induced per unit volume such as $Q = Q_h$ inside the NP and for the loss less materials $Q = 0$. In our computational study the values of κ, ρ and C_p are obtained from our previous reported work [5].

Water is chosen as base-fluid due its availability and high absorptivity in near-infrared range. For pure H_2O, the absorption effect is only important to be considered in our study due to negligible scattering. Therefore, spectral absorption coefficient (K_{H_2O}) of base-fluid can be calculated as [9].:

$$K_{H_2O} = \frac{4\pi k}{\lambda} \quad (3)$$

where k is index of absorption for water and λ is the wavelength of solar irradiation. The value of optical constant of base-fluid (water) is obtained from [29].

3. Results and discussion

3.1. Optical properties of plasmonic nanoassembly

The absorption and scattering cross-sections of the Au-NR assemblies (single nanorods N_1, dimers N_2, trimmers N_3, and tetramer N_4) are represented in Fig. 2. The dominant contribution to the LSPR absorption spectrum is due to dipole resonance, which is reliant on longitudinal oscillation mode.

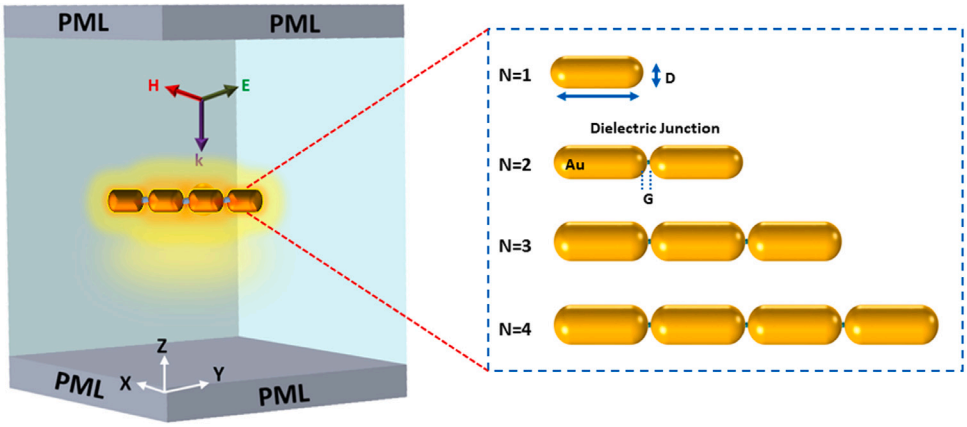

Fig. 1. Plasmonic nanostructures for single (N_1 = 1), dimer (N_2 = 2), trimer (N_3 = 3) tetramer (N_4 = 4) Au NR assembly bridged by dielectric material and computational domain.

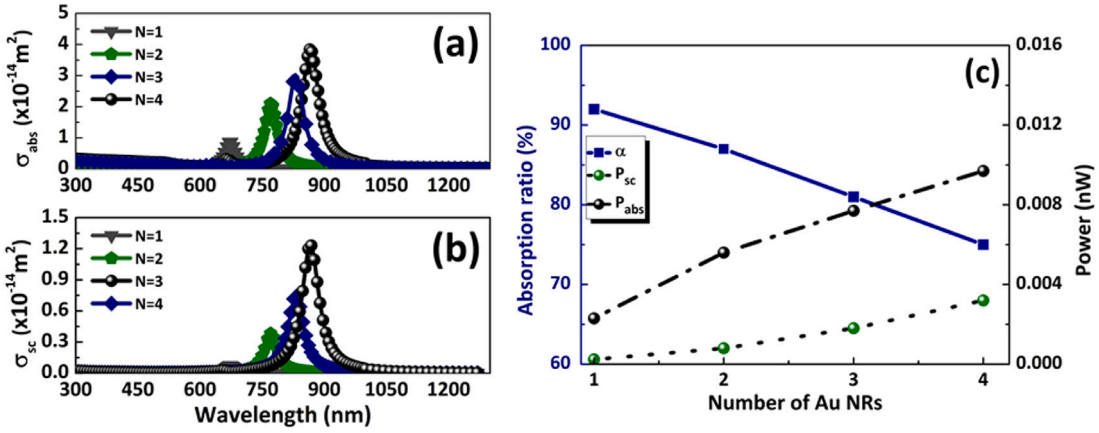

Fig. 2. (A) Absorption cross-section, (B) absorption ratio, α, power absorbed, Pabs, and power scattered, Psca, of the NR structures.

In order to evaluate the use of plasmonic chain in STC, Au nanofluids (NFs) contain single rod (N_1 = 1) and NR arrays (N_2 = 2, N_3 = 3 and N_4 = 4) were studied under the regime of low volume fraction ($p < 10^{-4}$). Fig. 2 displays the calculated FEM optical properties of Au-NR chain for tetramer (N_4), trimmers (N_3), dimers (N_2) assemblies and single nanorods (N_1). The dominant contribution to LSPR absorption spectrum is due to dipole resonance, which is reliant on longitudinal oscillation mode. The numerical calculations show that the absorption performance of Au-NRs chain enhance on increasing the assembly length (Fig. 2(a)).

In particular, the absorption efficiency grows nearly four times for the N_4 assembly as compared to an individual nanorod. On enlarging the NP assembly, a red-shift is observed on the LSPR spectrum. As the particle assembly increases, the contribution of both absorption and scattering cross sections increase in LSPR optical spectrum (Fig. 2a, b). However, the extinction cross-section is mainly determined by overall absorption contribution of the structures, as depicted by the absorption ratio values shown in Fig. 2(b). High values of absorption ratio are obtained for single NR (α = 92%) and dimers (α = 87%). For each additional nanorod linkage the absorption contribution for the extinction cross-section is reduced. The absorption ratio for N_4 is 76%, a value higher than the gold nanosphere with 50 nm radius (α = 45%) [6]. Fig. 2(b) also demonstrates the influence of scattering and absorption power to the total extinction power of the plasmonic nanostructure. The incident solar radiation intensity used on the calculations was 800 W/m^2. Specifically, the absorption power value for gold N_4 assembly is three times higher than the scattering contribution. Moreover, the Au NR (N_4) assembly shows an absorption cross section about 2.7 times higher than the one for single Au-NR (L = 88 nm, D = 15 nm) with peak at 900 nm.

The interaction of electromagnetic waves with NPs can lead to light scattering and to the generation of resisting heat, which are reliant on the real and imaginary value of NP's dielectric function. The power absorbed and scattered by a nanoparticle, P_{abs} and P_{sca} respectively, can be calculated as [30]:

$$P_{abs} = \int_{\lambda_{min}}^{\lambda_{max}} I(\lambda)\sigma_{abs}(\lambda)d\lambda, \tag{4}$$

and

$$P_{sc} = \int_{\lambda_{min}}^{\lambda_{max}} I(\lambda)\sigma_{sc}(\lambda)d\lambda, \tag{5}$$

where $I(\lambda)$ is the solar radiation intensity, σ_{sca} is the NP scattering cross section and σ_{abs} is the NP absorption cross section. Moreover, on the analyses of light-interaction with metallic nanoparticle, one can define the absorption ratio as [30]:

$$\alpha = \frac{P_{abs}}{P_{abs} + P_{sc}}, \tag{6}$$

which describes the absorption effectiveness on the overall optical process.

For a colloid with known nanoparticle concentration (CNPs) and single nanostructure volume (V_{NP}), the NP volume fraction (p) is define as $p = V_{NPs}/V_{fluid}$, where V_{fluid} is the NFs volume and V_{NPs} is the total volume of nanoparticles. A plethora of literature demonstrated the use of metallic NFs on solar collector possessing height of one or few centimeters and volume fractions at the orders of 10^{-6} and 10^{-4} [2].

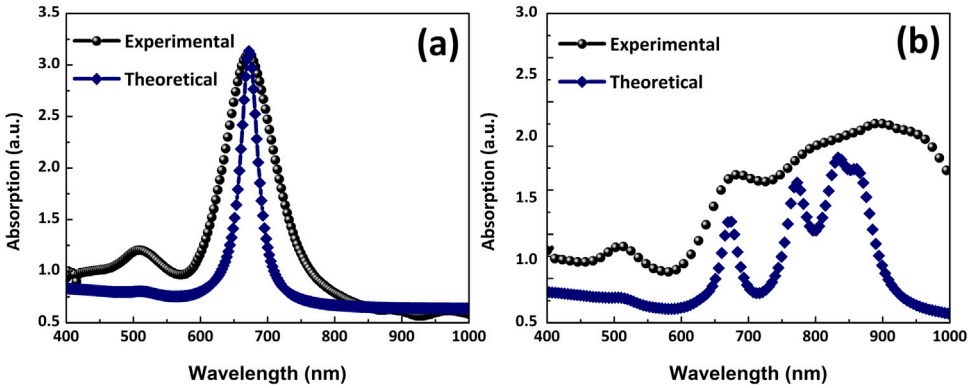

Fig. 3. Absorption spectra of single Au NR (a) and blended NFs (b) both experimentally [19] and theoretically in base-fluid (water) as a working fluid.

Thereby, here we defined a NF of volume $V_{fluid} = 1$ cm^3 (i.e. solar collector height 1 cm and illumination area of 1 cm^2). To estimate the efficiency of a direct absorption of a solar collector, the solar weighted absorption coefficient (A_m), which represents the percentage of the solar energy that is absorbed by the NF, were calculated. A_m is defined as [6]:

$$A_m = \frac{\int_{\lambda_{min}}^{\lambda_{max}} I_\lambda (1 - e^{-\sigma_{abs} C_{NPs} H}) dx}{\int_{\lambda_{min}}^{\lambda_{max}} I_\lambda dx}, \quad (7)$$

where I_λ is the spectral distribution of the solar intensity, H is the solar collector height. The term $I_\lambda(1-e^{-\sigma_{abs} C_{NPs} H})$ is named NF spectral absorbed irradiance, and accounts for the amount of sun power per unit of area that is absorbed by the colloid. Moreover, for an ideal solar radiation absorber, the A_m value is 1, which can be attained by increasing either the thickness (height) of the nanofluid or the nanoparticle concentration. The optimization of NF performance on a solar collector requires the analyzes of absorption efficiency parameters as σ_{abs}, P_{abs}, α and A_m.

Recently, Fontana et al. described the synthesis of gold nanorods chains [19,20]. Colloidal nanorods dimers, trimers and tetramers were formed in macroscale quantities. In summary, Au nanoparticle assemblies were performed by molecular-linking gold nanorods with 42 nm length and 15 nm diameter, with LSPR peaks at 670 nm (longitudinal mode) and 510 nm (transverse mode). As the nanorods begin to link together into linear chains a red-shifting was observed for each additional nanorod linkage, broadening the colloid spectrum. Peaks at 790 nm, 880 nm, 930 nm is identified on the absorption spectrum of the colloidal nanorods assembly [19,20]. In Fig. 3, the simulated resonance spectra of a single nanorod and a mixed inhomogeneous colloid are presented. The simulated blended colloidal (N-mixture) is composed of tetramer, trimmers, dimers and single nanorods, with 13%, 17%, 25% and 45% relative populations, respectively. The relative concentration were determined based on the experimental data of Ref. Fontana et al. [19]. The difference on the peaks position and width of the measured [19,20], and simulated spectra can be attributed to the fact that the plasmonic inhomogeneous mixture is composed by nonlinear chains, where angles between connected rods is observed [19,20]. Further, the Au NRs assembly will reinforce solar collector's long-wavelength absorption, governing a broad band absorption. In order to investigate the influence of the contribution of the blended NF, we compared the calculated absorption spectrum of the fluid with an experimental analysis and achieved the broadness of LSRP spectrum around 500 nm employing blended NFs, which is difficult to obtain with monomers.

3.2. Solar weighted absorption coefficient of nanofluids

As aforementioned in Section 3.1, the high efficient nanofluid for STC should present an absorption spectrum matching the solar radiation spectrum. Fig. 4(a) simultaneously shows the overlapped of the solar spectrum (i.e. ASTM G173-03 AM 1.5 Global) and the plasmonic inhomogeneous mixture (45% of N_1, 25% of N_2, 17% of N_3 and 13% of N_4) absorption spectrum, indicating that the inhomogeneous mixture is attractive as a nanofluid for STC. The influence of the nanofluid spectral absorbed irradiance relies on the colloidal gold volume fraction (p). Fig. 4(b) depicted the simulated spectral absorbed irradiance for different nanofluids (with $p = 5 \times 10^{-6}$). The solar spectrum i.e. ASTM G173-03 AM 1.5 Global can also be seen in Fig. 4(b). Fig. 4(b) indicates that NR tetramer and mixture NR assembly based colloid may present a high performance on harvesting solar radiation.

As aforementioned (Eq. (5)), the solar weighted absorption coefficient (A_m) of the nanofluid depends on the NPs geometry, the nanofluid thickness and nanoparticle concentration (or volume fraction). The A_m factor was calculated by employing Eq. (5) and integrating it from 300 nm to 1000 nm. It can be seen from Fig. 5 that A_m dependence on volume fraction of nanorod assembly based nanofluid with the thickness $H = 1$ cm and Au-NR homogeneous assembly, consisting of $N = 1$ to $N = 4$, and blended colloid (45% of N_1, 25% of N_2, 17% of N_3 and 13% of N_4). Fig. 5 shows that the nanofluid containing single nanorods (N_1) presents very low A_m factor i.e. 65% solar weighted absorption efficiency for $p = 10^{-5}$. However, under the same parameters, the A_m value grows as the NR chain increases. For instance, four-particle assembly presented an A_m value equal to 99%. Moreover, the blended nanofluid also shows a high A_m factor for $p = 10^{-5}$ reaching 97%. Table 1 presents the solar weighted absorption efficiency of blended nanofluids, reported in the literatures. On compering the solar weighted absorption coefficient of nanofluids attention should be given to the particle concentration (or volume fraction) of the nanostructure of the colloid. Cole et al. used a binary composition of gold nanoparticles with different shapes (nanosphere and nanoshell) to obtaining 84% absorption of the incident light [31]. More recently, Du and Thang proposed the use of plasmonic nanofluids based on a blend of gold nanorods with different aspect ratios (10% for AR = 1, 15% for AR = 3 and 75% for AR = 5) [32]. The computational simulations showed that, under 780 W/m^2 of solar flux, the blended nanofluid could absorb absorbed 580 W/m^2 of the solar power density. Several authors explored different materials in a blended nanofluid. Chen et al. reported a high performance nanofluid based on a mixture of SiO_2/Au and SiO_2/Ag core shell, obtaining a 94.4% Am value for $p \sim 10^{-5}$ [9]. Moreover, the use of distinct metal nanospheres (copper and gold) were proposed by Jin et al. and a 82% solar weighted absorption coefficient was achieved for 10^{-5} [33]. The photothermal conversion of a binary nanofluid of CuO and ZnO nanosphere were investigated by Fang et al. and for NPs volume fraction of 10^{-4} a $A_m = 94.78\%$ was demonstrated. [34]. The use of aluminum oxide and cobalt oxide were also evaluated for direct absorption SCT, and a low performance ($A_m \leq 70\%$ for $p \sim 10^{-5}$) of the blended nanofluid was observed [35].

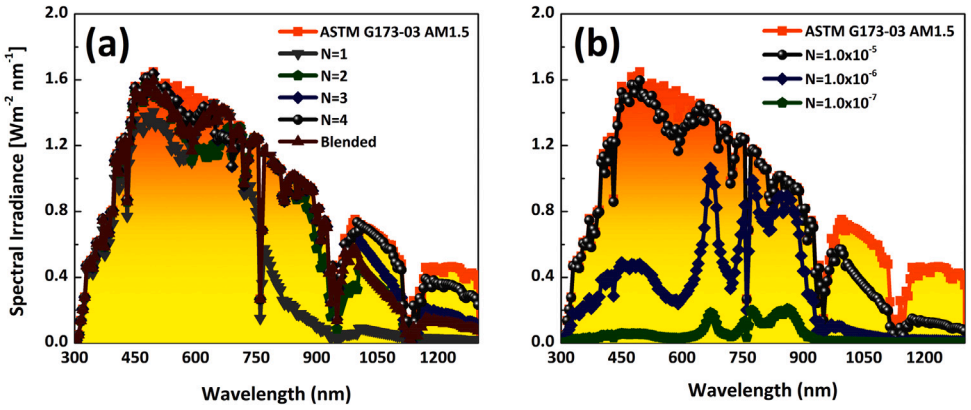

Fig. 4. (A) Solar spectral irradiance ASTM G173-03 AM1.5 and the plasmonic inhomogeneous mixture (blended) absorption spectrum, with 45% of N_1, 25% of N_2, 17% of N_3 and 13% of N_4. (B) The nanofluid spectral absorbed irradiance, for blended nanofluid with various concentrations when $H = 1$ cm.

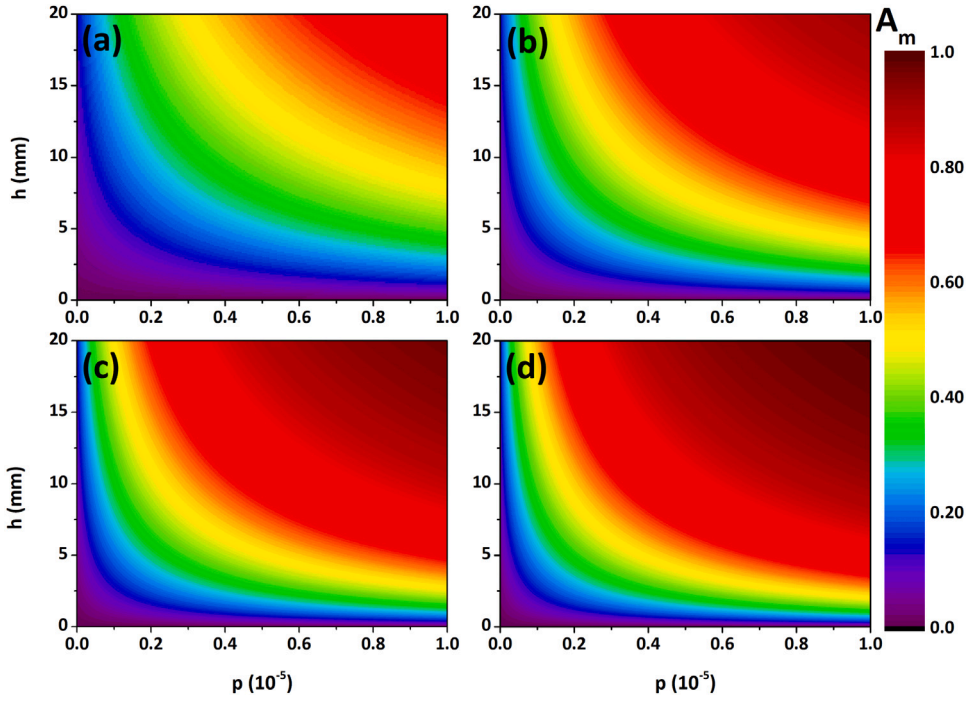

Fig. 5. Dependence of A_m factor on the gold volume friction of the nanofluid of Au NR assembly, with $N = 1$ to $N = 4$, and of the blended colloid (45% of N_1, 25% of N_2, 17% of N_3 and 13% of N_4).

Table 1
Survey of solar weighted absorption coefficient of various blended nanofluid for DASC.

Blend-structures	A_m	p	References
Au NR Assembly	97%	10^{-5}	This work
Au nanosphere and nanoshell	84%	–	[31]
Au NR (10% AR = 1, 15% AR = 3, 75% AR = 5)	74.3%	3×10^{-6}	[32]
Blended SiO2/Au and SiO2/Ag naoshell	94.4%	10^{-5}	[9]
Blended CuO and ZnO nanosphere	94.78	10^{-4}	[34]
Blended Al2O3 and Co3O4 nanosphere	70%	10^{-5}	[35]

3.3. Thermal analysis

In a STC, the light absorbed by the nanoparticles is converted into heat, increasing the temperature of the metallic nanostructure. The temperature (T) can be estimated by examining the diffusive heat flow equation for a homogeneous medium, given by [36]:

$$k\nabla^2 T + \frac{dQ}{dt} = c\frac{\partial T}{\partial t}, \tag{8}$$

where T is the temperature field, κ is the medium thermal conductivity, c is the medium heat capacity per unit volume, and $\frac{dQ}{dt}$ is the heat power density generated by nanoparticles. In water, the nanoparticle temperature reaches a steady state after 10 ns of light excitation. Chen et al. showed that, for different gold nanostructures (with volume $\sim 2.6 \times 10^5$ nm^3) embedded in water and irradiated by 10^5 suns, the nanoparticle temperature could increase up to 22 °C [37].

The steady-state temperature for the NR assemblies, for a 10 μs excitation under 10^5 suns, is presented in Fig. 6. The calculated model based FEM simulations consisted of an individual particle to Au-NR assembly. Considering the regime of low volume fraction ($p < 10^{-4}$), the change in temperature across the boundary of the FEM simulations unit cell was negligible. The high absorption cross-section of the Au-NR chain led to a significant enhancement of the nanostructure temperature. One can see that on enlarging the Au-NRs chain in colloid, there is a continuous increase in $\triangle T$. For instance, for monomer structure the $\triangle T$ varies from 0 to 7.7 °C. However, a rapid increase in temperature can be seen for dimeric structure till 24 °C. Similarly, the temperature

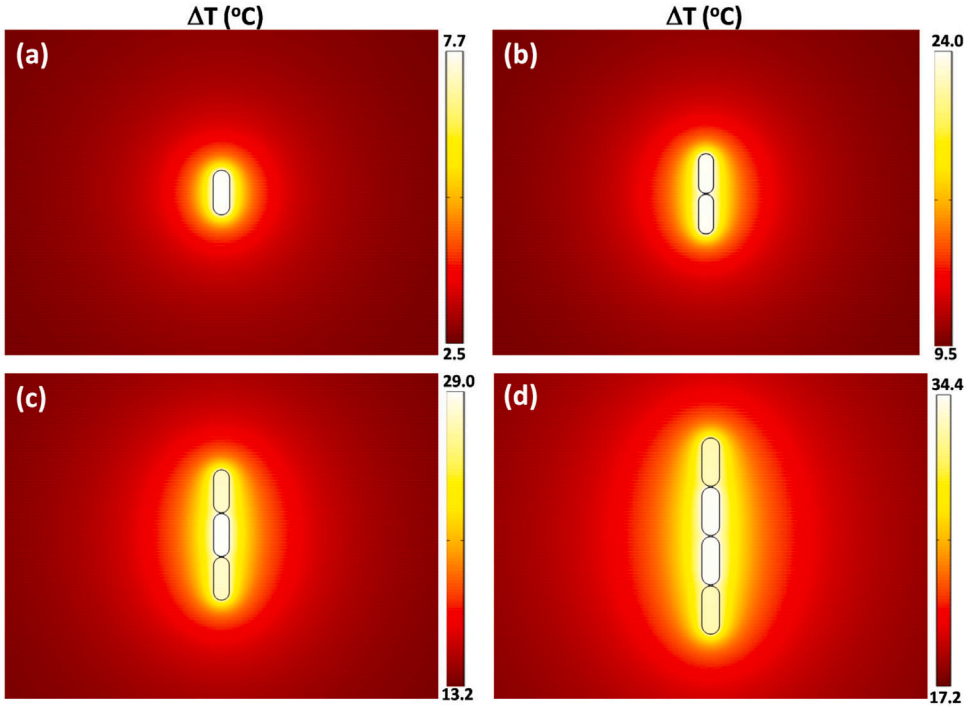

Fig. 6. Temperature increases of Au NR assemblies. The temperature profile is obtained by solar radiation (10^5 suns) at 10 μs.

variation was noticed up to 29 °C for Au NR trimer. Moreover, in particular, the calculated steady-state temperature increases of the N_4 chain was 34.4 °C, 4.4× higher than the single NR. Although, N_4 structure presents a volume (2.5×10^4 nm^3) 10-times smaller than the structures (sphere, cube and cylinder), the temperature increase observed on the Au-NR chain is 53% higher than the ones reported by Chen et al. [37]. On considering a solar excitation of 1 sun, the temperature increase of a single gold nanostructure is negligible (lower than 10^{-3} °C). However, the continuum heating of a dispersed nanoparticle assemble can lead to a significant enhancement of the global colloid temperature. The time scale for heat diffusion across 1 cm in the colloid can be estimated about 1000 s (typical solar excitation time on a STC system). For 1 cm^3 heated volume with $p = 10^{-5}$, 10^6 randomly dispersed Au-NRs will contribute to the global temperature of the colloidal volume. Considering the NPs as a homogeneous heat source distributed in the heated region, the superposition of the temperature field of each NP will lead to the enhancement of the colloid temperature, given by [36]

$$\frac{\triangle T_{Colloid}}{\triangle T_{NP}} = \left(\frac{R}{r_{NP}}\right)^2 \times p, \tag{9}$$

where r_{NP} and R are the nanoparticle and heated volume equivalent radius, respectively.

Fig. 7 shows the nanofluid temperature under (time = 100 μs) 1 sun excitation, for different nanoparticle ensembles. The results indicate that tetramer based nanofluid can reach a temperature of 58.45 °C, more than 10× higher than single-nanorods colloid. Although these values of the solar collector operating under specified Au-NRs structures are yet to be considered a considerable improvement, the NFs given in this work are much better than those previously reported literature (Table 1). Still, there exists plenty of room for further improvement. Considering novel nanostructures and their broad spectrum, the present work clearly depicts the advantages of using the plasmonic blended nanofluid as a working fluid in a DASC. Further, by coupling as well as confining light, plasmonic Au-NRs assembly provides exceptional opportunities to sense and signal at nanoscale for energy harvesting at large, and in biomedical applications.

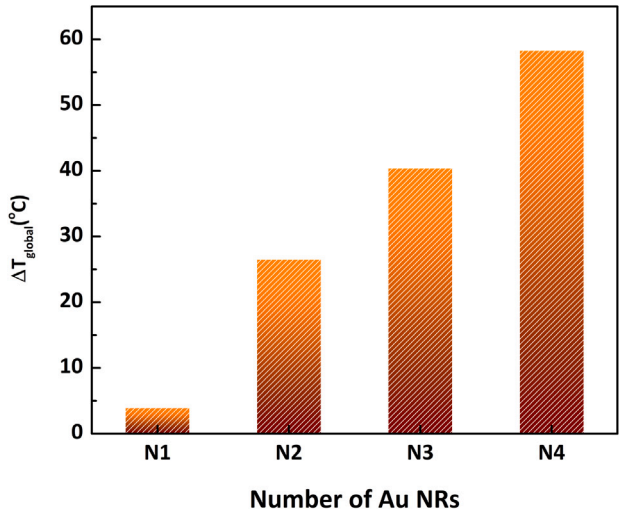

Fig. 7. Solar thermal efficiencies of different nanofluids under 1 sun illumination at 100 μs.

4. Conclusion

The performance of gold nanorods assembly in nanofluids for direct solar thermal collector was evaluated. The enlarging the Au-NR assembly enhances the absorption performance and ultimately increases solar weighted absorption coefficient of the nanofluid. The obtained A_m values are close to the ideal solar thermal collector condition ($A_m = 1$). Blended nanofluid based on nanorod-chain was evaluated indicating a high performance of the composed colloid on harvesting solar energy. The temperature increase of the colloid exposed to 1 sun excitation reached more than 55 °C, for the tetramer nanofluid. Therefore, the nanofluids based on Au-NRs assembly show the emerging potential to be explored in STC as a nanofluid.

Declaration of competing interest

The authors declare that they have no known competing financial interests or personal relationships that could have appeared to influence the work reported in this paper.

Data availability

Data will be made available on request.

Acknowledgments

This work was supported by the Office of Naval Research Global (Award N62909-18-1-2099) and the Brazilian Agencies CNPq, CAPES and FACEPE. The authors also acknowledges the support of the Polytechnic School of Pernambuco. Dr. Zafar Said would like to thank the University of Sharjah, (Award 22020405195), for its financial support.

References

[1] J. Koschikowski, M. Wieghaus, M. Rommel, Solar thermal-driven desalination plants based on membrane distillation, Desalination 156 (1–3) (2003) 295–304.
[2] T.P. Otanicar, P.E. Phelan, R.S. Prasher, G. Rosengarten, R.A. Taylor, Nanofluid-based direct absorption solar collector, J. Renew. Sustain. Energy 2 (3) (2010) 033102.
[3] R. Shende, R. Sundara, Nitrogen doped hybrid carbon based composite dispersed nanofluids as working fluid for low-temperature direct absorption solar collectors, Sol. Energy Mater. Sol. Cells 140 (2015) 9–16.
[4] M. Seyednezhad, M. Sheikholeslami, J.A. Ali, A. Shafee, T.K. Nguyen, Nanoparticles for water desalination in solar heat exchanger, J. Therm. Anal. Calorim. (2019) 1–18.
[5] Z. Said, S. Arora, S. Farooq, L.S. Sundar, C. Li, A. Allouhi, Recent advances on improved optical, thermal, and radiative characteristics of plasmonic nanofluids: Academic insights and perspectives, Sol. Energy Mater. Sol. Cells (2021) 111504.
[6] S. Farooq, C.V.P. Vital, L.A. Gómez-Malagón, R.E. de Araujo, D. Rativa, Thermo-optical performance of iron-doped gold nanoshells-based nanofluid on direct absorption solar collectors, Sol. Energy 208 (2020) 1181–1188.
[7] J.E. Minardi, H.N. Chuang, Performance of a "black" liquid flat-plate solar collector, Sol. Energy 17 (3) (1975) 179–183.
[8] M. Chen, Y. He, J. Huang, J. Zhu, Investigation into Au nanofluids for solar photothermal conversion, Int. J. Heat Mass Transfer 108 (2017) 1894–1900.
[9] M. Chen, Y. He, X. Wang, Y. Hu, Complementary enhanced solar thermal conversion performance of core-shell nanoparticles, Appl. Energy 211 (2018) 735–742.
[10] T.P. Otanicar, P.E. Phelan, J.S. Golden, Optical properties of liquids for direct absorption solar thermal energy systems, Sol. Energy 83 (7) (2009) 969–977.
[11] C.V.P. Vital, S. Farooq, R.E. de Araujo, D. Rativa, L.A. Gómez-Malagón, Numerical assessment of transition metal nitrides nanofluids for improved performance of direct absorption solar collectors, Appl. Therm. Eng. 190 (2021) 116799.
[12] I. Carrillo-Berdugo, J. Sampalo-Guzmán, R. Grau-Crespo, D. Zorrilla, J. Navas, Interface chemistry effects in nanofluids: Experimental and computational study of oil-based nanofluids with gold nanoplates, J. Molecular Liquids (2022) 119762.
[13] J. Buongiorno, D.C. Venerus, N. Prabhat, T. McKrell, J. Townsend, R. Christianson, Y.V. Tolmachev, P. Keblinski, L.-w. Hu, J.L. Alvarado, et al., A benchmark study on the thermal conductivity of nanofluids, J. Appl. Phys. 106 (9) (2009) 094312.
[14] A.J. Moghadam, M. Farzane-Gord, M. Sajadi, M. Hoseyn-Zadeh, Effects of CuO/water nanofluid on the efficiency of a flat-plate solar collector, Exp. Therm Fluid Sci. 58 (2014) 9–14.
[15] T. Yousefi, F. Veysi, E. Shojaeizadeh, S. Zinadini, An experimental investigation on the effect of Al2O3–H2O nanofluid on the efficiency of flat-plate solar collectors, Renew. Energy 39 (1) (2012) 293–298.
[16] H. Tyagi, P. Phelan, R. Prasher, Predicted efficiency of a low-temperature nanofluid-based direct absorption solar collector, J. Sol. Energy Eng. 131 (4) (2009).
[17] E.P. Bandarra Filho, O.S.H. Mendoza, C.L.L. Beicker, A. Menezes, D. Wen, Experimental investigation of a silver nanoparticle-based direct absorption solar thermal system, Energy Convers. Manage. 84 (2014) 261–267.
[18] M. Chen, Y. He, J. Zhu, D.R. Kim, Enhancement of photo-thermal conversion using gold nanofluids with different particle sizes, Energy Convers. Manage. 112 (2016) 21–30.
[19] J. Fontana, R. Nita, N. Charipar, J. Naciri, K. Park, A. Dunkelberger, J. Owrutsky, A. Piqué, R. Vaia, B. Ratna, Widely tunable infrared plasmonic nanoantennas using directed assembly, Adv. Opt. Mater. 5 (21) (2017) 1700335.
[20] J. Fontana, N. Charipar, S.R. Flom, J. Naciri, A. Pique, B.R. Ratna, Rise of the charge transfer plasmon: Programmable concatenation of conductively linked gold nanorod dimers, ACS Photonics 3 (5) (2016) 904–911.
[21] B. Gerislioglu, L. Dong, A. Ahmadivand, H. Hu, P. Nordlander, N.J. Halas, Monolithic metal dimer-on-film structure: New plasmonic properties introduced by the underlying metal, Nano Lett. 20 (3) (2020) 2087–2093.
[22] A. Yadav, B. Gerislioglu, A. Ahmadivand, A. Kaushik, G.J. Cheng, Z. Ouyang, Q. Wang, V.S. Yadav, Y.K. Mishra, Y. Wu, et al., Controlled self-assembly of plasmon-based photonic nanocrystals for high performance photonic technologies, Nano Today 37 (2021) 101072.
[23] P.B. Johnson, R.-W. Christy, Optical constants of the noble metals, Phys. Rev. B 6 (12) (1972) 4370.
[24] K. Liu, X. Xue, E.P. Furlani, Theoretical comparison of optical properties of near-infrared colloidal plasmonic nanoparticles, Sci. Rep. 6 (2016) 34189.
[25] S. Farooq, F. Wali, D.M. Zezell, R.E. de Araujo, D. Rativa, Optimizing and quantifying gold nanospheres based on LSPR label-free biosensor for dengue diagnosis, Polymers 14 (8) (2022) 1592.
[26] S. Farooq, D. Rativa, R.E. de Araujo, Orientation effects on plasmonic heating of near-infrared colloidal gold nanostructures, Plasmonics 15 (5) (2020) 1507–1515.
[27] S. Farooq, D. Rativa, R.E. de Araujo, High performance gold dimeric nanorods for plasmonic molecular sensing, IEEE Sens. J. (2021).
[28] M. Khademalrasool, M.D. Talebzadeh, Rapid synthesis of silver nanowires during the polyol-microwave method and COMSOL multiphysics simulation of electromagnetic heating, Adv. Powder Technol. 32 (8) (2021) 2916–2928.
[29] G.M. Hale, M.R. Querry, Optical constants of water in the 200-nm to 200-μm wavelength region, Appl. Opt. 12 (3) (1973) 555–563.
[30] X. Chen, P. Zhou, M. Chen, Enhancing the solar absorption performance of nanoparticle suspensions by tuning the scattering effect and incident light location, Int. J. Therm. Sci. 177 (2022) 107547.
[31] J.R. Cole, N.J. Halas, Optimized plasmonic nanoparticle distributions for solar spectrum harvesting, Appl. Phys. Lett. 89 (15) (2006) 153120.
[32] M. Du, G.H. Tang, Plasmonic nanofluids based on gold nanorods/nanoellipsoids/nanosheets for solar energy harvesting, Sol. Energy 137 (2016) 393–400.
[33] X. Jin, G. Lin, A. Zeiny, H. Jin, L. Bai, D. Wen, Solar photothermal conversion characteristics of hybrid nanofluids: An experimental and numerical study, Renew. Energy 141 (2019) 937–949.
[34] J. Fang, Y. Xuan, Investigation of optical absorption and photothermal conversion characteristics of binary CuO/ZnO nanofluids, RSC Adv. 7 (88) (2017) 56023–56033.
[35] V. Bhalla, V. Khullar, H. Tyagi, Experimental investigation of photo-thermal analysis of blended nanoparticles (Al2O3/Co3O4) for direct absorption solar thermal collector, Renew. Energy 123 (2018) 616–626.
[36] P. Keblinski, D.G. Cahill, A. Bodapati, C.R. Sullivan, T.A. Taton, Limits of localized heating by electromagnetically excited nanoparticles, J. Appl. Phys. 100 (5) (2006) 054305.
[37] M. Chen, Y. He, X. Wang, Y. Hu, Numerically investigating the optical properties of plasmonic metallic nanoparticles for effective solar absorption and heating, Sol. Energy 161 (2018) 17–24.